Article

Visible Light-Induced Metal Free Surface Initiated Atom Transfer Radical Polymerization of Methyl Methacrylate on SBA-15

Liang Ma [1], Na Li [1,*], Jian Zhu [2] and Xiaodong Chen [1]

[1] College of Chemistry, Chemical Engineering and Materials Science, Soochow University, Suzhou 215123, China; lma49@stu.suda.edu.cn (L.M.); xdchen@mail.suda.edu.cn (X.C.)

[2] Jiangsu Key Laboratory of Advanced Functional Polymer Design and Application, State and Local Joint Engineering Laboratory for Novel Functional Polymeric Materials, College of Chemistry, Chemical Engineering and Materials Science, Soochow University, Suzhou 215123, China; chemzhujian@suda.edu.cn

* Correspondence: chemlina@suda.edu.cn; Tel.: +86-512-65882752

Abstract: Surface initiated atom transfer radical polymerization (SI-ATRP) is one of the most versatile technique to modify the surface properties of material. Recent developed metal free SI-ATRP makes such technique more widely applicable. Herein photo-induced metal-free SI-ATRP of methacrylates, such as methyl methacrylate, N-isopropanyl acrylamide, and N,N-dimethylaminoethyl methacrylate, on the surface of SBA-15 was reported to fabricate organic-inorganic hybrid materials. SBA-15 based polymeric composite with adjustable graft ratio was obtained. The structure evolution during the SI-ATRP modification of SBA-15 was monitored and verified by FT-IR, XPS, TGA, BET, and TEM. The obtained polymeric composite showed enhanced adsorption ability for the model compound toluene in aqueous. This procedure provides a low cost, ready availability, and facile modification way to synthesize the polymeric composites without the contamination of metal.

Keywords: polymeric composite; surface initiated atom transfer radical polymerization; photo-induced; living radical polymerization; metal-free atom transfer radical polymerization

1. Introduction

Functionalization of mesoporous silica materials such as MCM-n, HMS-n, and SBA-n with organic groups has attracted considerable research interest in the past few years[1-6]. In particular, ordered mesoporous materials such as SBA-15 are ideal candidates for functionalization due to their high hydrothermal stability, desired morphology, adjustable pore sizes (2–30 nm), and thick walls that can be easily functionalized using silanol chemistry[7, 8]. In this context, the covering of a silica surface with different polymers seems to be a potentially useful strategy for incorporating a range of organic functional groups which could modify the properties of these materials and open up new fields for novel applications. The properties of the resulting surface are governed by the type and amount of polymer used in the process, which evidently enriched the functional modification of these materials.

Surface-initiated polymerizations are the most frequently used methods to covalently connect polymer chains to the surface of a material, which are based on the so-called "grafting from" technique[9, 10]. Significant advances in this area have been achieved by the development of living radical polymerization techniques, especially as nitroxide-mediated polymerization (NMP)[11, 12], reversible addition-fragmentation chain transfer polymerization (RAFT)[13], and atom transfer radical polymerization (ATRP)[14]. Among them, surface initiated atom-transfer radical polymerization (SI-ATRP) has been received much of attentions during the past two decades[2, 15-18]. So far, polymers with controlled structures and functional side groups can be grafted on various surfaces by SI-ATRP, such as antifouling coatings[19], drug delivery[20], stimuli-responsive materials[21], and nanoporous membranes[22].

Originally, ATRP[23-27] was carried out with relatively high concentrations of transition metals, typically the Cu-based catalyst, in order to compensate for unavoidable radical termination reactions. Recently, several systems were developed that enabled ATRP to proceed at a catalyst loading of only 10−100 ppm of Cu[28, 29]. This occurs in the presence of various reducing agents that continuously regenerate Cu^{+} activators from Cu^{2+} deactivators and compensates for radical termination. Although catalyst loadings can be decreased to parts per million (ppm), for a variety of applications, such as microelectronics, biomaterials, etc., a key limiting factor in using ATRP is metal contamination. Very recently, Hawker et.al[30] reported a photo-induced metal-free ATRP of methyl methacrylate using 10-phenylphenothiazine (PTH) as an organic photocatalyst. In this photo-induced, metal-free ATRP mechanism, a three component photoredox cycle is conducted. The photoexcited PTH* activates an alkyl halide and generates radicals, while the PTH+•Br− specie deactivates the radical and regenerates the ground state PTH. Latterly, the metal-free ATRP system has been developed very fast. Various catalyst systems with improved control abilities were developed in these years[31-33]. With these development, metal-free SI-ATRP also has been verifies in recent years. However, these reports were focused on the modification surface properties of flat surfaces and particles by SI-ATRP[34, 35]. Seldom examples of metal-free SI-ATRP on the surface of mesoporous material were reported.

Herein we report a procedure to synthesize organic-inorganic hybrid materials based on photo-induced metal-free SI-ATRP of methacrylate monomers on the surface of SBA-15. The ATRP initiator is chemically bound to the mesostructure walls beforehand such that polymer growth occurs directly from and over the SBA- 15 internal surface. This procedure provides a low cost, ready availability, and facile modification way to synthesize the polymeric composites without the contamination of metal.

2. Materials and Characterization

Materials

(3-aminopropyl)triethoxysilane (APTES) was purchased from Shanghai MACKLIN Reagent Co., Ltd. and used as received. Methyl methacrylate (MMA) (Shanghai Chemical Reagents Co. Ltd., China) was purified before use by passing through a column filled with neutral aluminum oxide. Triethylamine (TEA, Chinasun Specialty Products Co. Ltd., China) was dried with 4 Å molecular sieves and distilled before use. Pluronic 123 was purchased from Sigma-Aldrich (Shanghai) Co., Ltd. and used as received. Tetraethlorthosilicate (TEOS), hydrochloric acid (HCl), 2-bromoisobutyl bromide (BMBP), were also purchased from Shanghai Chemical Reagents Co., Ltd. and used as received. Solvents, dimethylformamide (DMF) and tetrahydrofuran (THF) were purchased from Shanghai Chemical Reagents Co., Ltd. and purified by standard methods.

Synthesis of SBA-15

SBA-15 was synthesized according to the procedure reported by Zhao et al[7] using Pluronic 123 triblock copolymer as a template. Briefly, 20 g of Pluronic 123 was dissolved under stirring in 600 mL of 2M HCl and 150 mL of deionized water at 40 ℃. Then 42.5 g of tetraethlorthosilicate (TEOS) was [8]added. The resultant solution was stirred for 24 h at 40 ℃ before transferring into a Teflon bottle sealed in an autoclave, which was then heated to 130 ℃ for 24 h in an oven. The solid product was recovered by filtration and dried at 40 ℃ for 5 h in the vacuum oven. The template was removed from the as-made mesoporous material by calcination at 550 ℃ for 5 h (heating rate is 1.5 ℃/min).

Synthesis of SBA-APTES

Amount of 8.0 g calcined SBA-15 was degassed under vacuum at 40 ℃ overnight before added into a three-necked flask containing 350 mL of dry toluene and 8 mL of (3-aminopropyl)triethoxysilane (APTES). The mixture was stirred for 5 h under reflux at a nitrogen atmosphere. Under this condition, the hydroxyl groups of the SBA-15 surface react with the ethoxy groups of the APTES molecules, resulting an amino-functionalized SBA-APTES. Then, the solid was recovered by filtration and intensively washed with toluene before dried under vacuum at 40 ℃ overnight.

Synthesis of SBA-Br

Compound 2-bromo-2-methylpopionyl bromide (BMPB) was used to react with the previously attached aminopropyl groups leading the ATRP initiator bonded on SBA-15 pores surface. In this case, 8.6 g of the functionalized SBA-15 material was added to a three-necked flask containing 300

mL of dry toluene and 9 mL triethylamine. Then, 8 mL of BMPB was added in a constant pressure funnel. The system was stirred for 3 h under reflux and a nitrogen atmosphere. Finally, the solid was recovered by filtration, washed with deionized water until the filtrate was clear, and outgassed under vacuum at 40 ℃ overnight.

Synthesis of SBA-PMMA

A typical experimental procedure for SBA-PMMA by metal-free photo-induced SI-ATRP follows: 1mL of methyl methacrylate(MMA, 0.9440 g, 9.43 mmol, 100 equiv), 18.4 mg of ethyl 2-bromoisobutyrate(EBiB, 0.09 mmol, 1 equiv), 5.0 mg of 10-phenylphenothiazine(PTH, 0.02 mmol, 0.2 equiv), 1.0 g of SBA-Br, and 1 mL of DMF were added to an ampoule. The ampoule was tightly sealed and oxygen was removed by three freeze-pump-thaw cycles. The reaction was irradiated under a 3.0 mW/cm2 xenon lamp with the 380 nm optical filter. After a predetermined time, the ampoule was removed from the irradiation and the reaction mixture was then diluted with THF and centrifuged(10,000 rpm, 10 min) to collect the polymer-grafted SBA-15. The centrifugation and redispersion was repeated three times. The number-average molecular weight Mn and dispersity (Mw/Mn) were obtained by GPC using linear PMMA standards in THF as the eluent. The graft density was calculated gravimetrically. The obtained samples were denoted as SBA-PMMA.

Batch adsorption

The liquid phase adsorption was ultrasoniced for 30 min and stirred for 2 h in 40 mL glass vails filled with 0.02 g of adsorbent and 10 mL of adsorbate solution which contains toluene in water with a concentration of 47 ppm. After the desired time was reached, the mixture was filtered by a nylon membrane filter (0.22 μm), then the mixture was analysed by GC. The concentration of adsorbate C_e was calculated as the formulation followed:

$$C_e = \frac{C_0}{\frac{A_0}{A_e}} \quad (1)$$

where C_0 is the concentration of the initial adsorbate solution; A_0 and A_e are the GC areas of initial adsorbate solution and treated solution, respectively.

Characterization

Fourier transform infrared spectroscopy(FT-IR) spectra were recorded on a TENSOR 27, BRUKER Optik GmbH, Germany. TGA was carried out on PerkinElmer PYRIS 1 TGA thermogravimetric analyzer at a heating rate of 10 ℃ min^{-1} from room temperature to 700 ℃ in a nitrogen atmosphere. Surface compositions were determined by X-ray photoelectron spectroscopy(XPS) on a KRA70S AXIS Ultra DLD spectrometer at a pressure of ≈2×10^{-8} Torr using Al Kr radiation as the exciting source; the instrument was operated at 15 kV and 10 mA. The surface area was determined via the nitrogen adsorption/desorption technique at 77 K using the ASAP 2020 surface area and porosimetry analyzer. The standard BET and DFT models were applied to determine the surface area and pore volume. The number-average molecular weight ($M_{n,GPC}$) and molecular weight distribution ($Đ$) of the polymers were determined by a TOSOH HLC-8320 equipped with a refractive-index detector, using a TSKgel guard column SuperMP-N (4.6×20 mm) and two TSKgel Supermultipore HZ-N (4.6×150 mm) with a measurable molecular weight ranging from 5×10^2 to 5×10^5 g/mol. DMF (+LiBr 0.1% weight) was used as the eluent at a flow rate of 0.6 mL/min and 40°C. GPC samples were injected using a TOSOH plus auto sampler and calibrated with PS standards purchased from TOSOH. The concentration of toluene in the treated solution was quantitatively analysed using a GC2010 (Shimadzu) plus gas chromatography with a low-polarity capillary column and a flame ionization detector (FID). The oven temperature was initially set at 80 ℃, and held this temperature for 5 min, then ramped at 5 ℃ min^{-1} to 140 ℃, and held at this temperature for 2 min. The temperatures of injector and detector were at 280 ℃ and 300 ℃ respectively.

3. Results

The SI-ATRP using functionalized SBA-15 as the initiator was carried out under the visible light irradiation with the presence of PTH. The synthetic route was showed in Scheme 1, which was similar to the literature[3, 30]. Thus, in order to carry out the SI-ATRP on the surface of SBA-15, the initiator moiety should be firstly anchored onto the surface of the

Preprints (www.preprints.org) | NOT PEER-REVIEWED | Posted: 22 January 2017 doi:10.20944/preprints201701.0095.v1

Peer-reviewed version available at Polymers 2017, 9, 58; doi:10.3390/polym9020058

material. Then, the photo-induced SI-ATRP was carried out. The FT-IR was used to monitor the structure evolution during such processing. The results were showed in Figure 1. Pristine SBA-15 showed a strong peak at 3440 cm^{-1}, corresponding to Si-OH stretching vibrations. After introduction of the initiator, peaks corresponding to C-H stretching vibrations at 2980 and 2920 cm^{-1}, -NH-CO- vibrations at 1535 cm^{-1}, and C-Br vibrations at 800 cm^{-1} were observed in the spectrum of SBA-Br. Such results implied the successfully introducing of the ATRP initiator functional moiety onto the surface of SBA-15 by silanol chemistry followed with the amidation reaction.

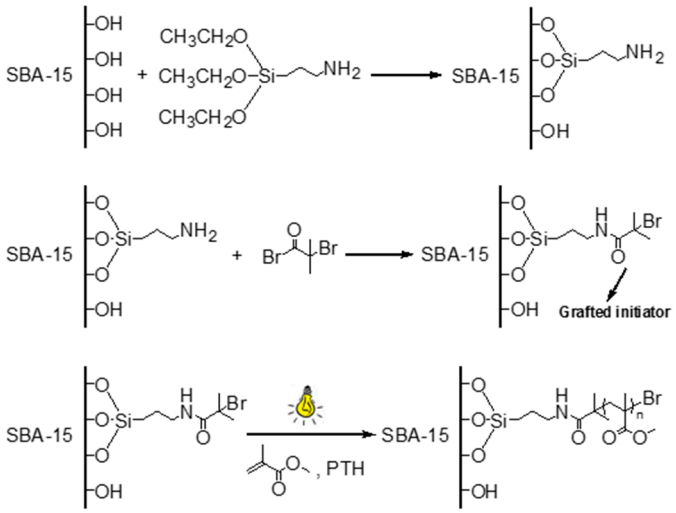

Scheme1. Synthetic procedure of the SBA-PMMA.

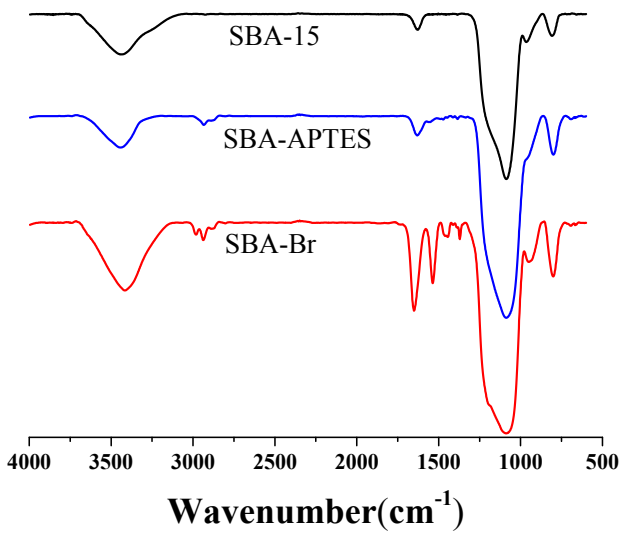

Figure 1. FT-IR spectra of SBA-15, SBA-APTES, and SBA-Br.

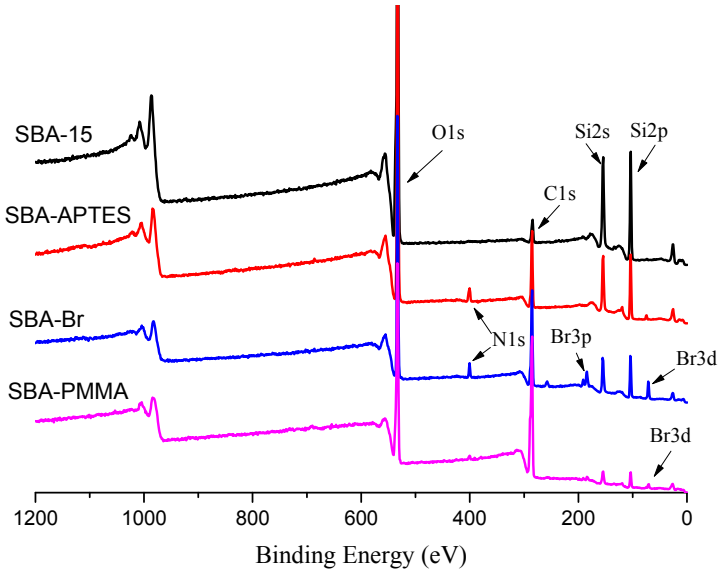

Figure 2. XPS spectra of SBA-15, SBA-APTES, SBA-Br, and SBA-PMMA.

For further confirm the surface structure, the materials obtained in different stages were characterized by XPS. The wide scan spectra of SBA-15, SBA-APTES, SBA-Br, and SBA-PMMA were summarized in Figure 2. It showed that the signal according to nitrogen was observed after SBA-15 treatment with 3-aminopropyltriethoxysilane (APTES). Such result indicated the successful anchored the APTES onto the surface of SBA-15. The signals according to nitrogen and bromine atoms were found in the XPS survey after SBA-APTES treating with 2-bromoisobutyryl bromide (BMPB), which implied the successful reaction between the surface amine groups with BMPB. Combined with the results of FT-IR, it clearly showed the successful introduction of ATRP initiating groups onto the surface of SBA-15. Furthermore, after the SI-ATRP of methyl methacrylate (MMA), the signals of nitrogen and bromine still remained in the spectrum, while the intensity was weakening, which implied the successfully surface initiated polymerization.

After these initial survey, the polymerizations of different monomers, e.g. MMA, DMAEMA, and NIPAM, were carried out using SBA-Br as the initiator, ethyl 2-bromoisobutyrate (EBiB) as the co-initiator and PHT as the photo catalyst under the irradiation of xenon lamp with the 380 nm optical filter at 30°C. The light intensity was 3.0 mW/cm^2. The polymerization results were summarized in Table 1. The molecular weight of the PMMA obtained in solution was measured by GPC using THF as the eluent and calibrated by PMMA standards. The molecular weights of the DMAEMA and NIPAM were measured by GPC using DMF as the eluent and calibrated by PMMA standards. It showed that non polymerization happened without the light irradiation or PTH after 72 hrs at 30°C (Entries 1 and 2 in Table 1). The polymerization could be carried out smoothly after adding PTH as the photo catalyst under the light irradiation (Entries 3-9 in Table 1). As high as 57.6% monomer conversion could be obtained after 72 hrs polymerization (Entry 7 in Table 1). The grafting ratio of the polymer was reached as high as 27.6%, which was similar as the literature results[36]. Not only the monomer MMA could be grafted onto the surface of SBA-15, but also monomers PDMAEMA and PNIPAM could be grafted onto the surface of SBA-15 (Entries 8 and 9 in Table 1), which implied the various applicable for current method to grafting polymers from the surface of SBA-15. The polymerization showed controlled characteristics, e.g. controllable molecular weights along with narrow molecular weight distribution of the obtained polymers.

Preprints (www.preprints.org) | NOT PEER-REVIEWED | Posted: 22 January 2017 doi:10.20944/preprints201701.0095.v1

Peer-reviewed version available at Polymers 2017, 9, 58; doi:10.3390/polym9020058

Table 1 Results of photo-induced metal-free SI-ATRP of MMA using SBA-Br as an initiator [a].

Entry	Label	Time (h)	Conv. (%)	$M_{n,GPC}$[d,e] (g/mol)	$Đ$[d,e]	Grafting ratio[f] (%)
1	[b] SBA-PMMA-C1	72.0	--	--	--	--
2	[c] SBA-PMMA-C2	72.0	--	--	--	--
3	SBA-PMMA-1	15.0	10.8	12800	1.24	12.5
4	SBA-PMMA-2	24.0	9.4	11100	1.29	21.6
5	SBA-PMMA-3	36.0	20.0	13300	1.28	24.6
6	SBA-PMMA-4	48.0	20.7	12800	1.24	25.0
7	SBA-PMMA-5	72.0	57.6	16700	1.27	27.6
8	[e] SBA-DMAEMA	20.0	83.4	21100	1.83	23.8
9	[e] SBA-NIPAM	18.0	85.0	13400	2.25	14.4

[a] $[monomer]_0/[EBiB]_0/[PTH]_0$ = 100/1/0.2; SBA-Br = 0.1 g. Polymerized at 30°C

[b] Without UV irradiation. $[monomer]_0/[EBiB]_0/[PTH]_0$ = 100/1/0.2; SBA-Br = 0.1 g.

[c] With UV irradiation. $[monomer]_0/[EBiB]_0/[PTH]_0$ = 100/1/0; SBA-Br = 0.1 g.

[d,e] Molecular weight of free polymers obtained from the solution determined by GPC using narrow poly(methyl methacrylate) standards, THF as the eluent. The molecular weight of PDMAEMA and PNIPAM were determined by GPC using narrow poly(methyl methacrylate) standards, DMF as the eluent.

[f] The grafting ratio was referred to the weight percentage of polymer to SBA-15 which was measured by TGA.

The photo-induced metal-free SI-ATRP on the surface of SBA-15 of different monomers were also monitored by TGA. The TGA curves of SBA-15, SBA-APTES, SBA-Br, SBA-PMMA at different conversions, SBA-DMEAME, and SBA-NIPAM were showed in Figure 3. The polymer chains started to decompose at 250 ℃ in a nitrogen atmosphere due to the elimination of ester group in the polymer chains. It showed that the amount of weight loss increased with polymerized time. Such results implied that the amount of polymer grafted on SBA-15 increased with the polymerized time. The grafting percentages of polymer on the surface of SBA-15 could be calculated from the TGA data, and were shown in Table 1. The grafting ratio could be varied in the range of 12.5% ~ 27.6% by changing the polymerization time, which offered the convenient way to adjust the amount of polymers on the surface of SBA-15. The grafting ratio of current system was slightly lower than the results reported in the literature, which may be caused by the porous structure of SBA-15[37].

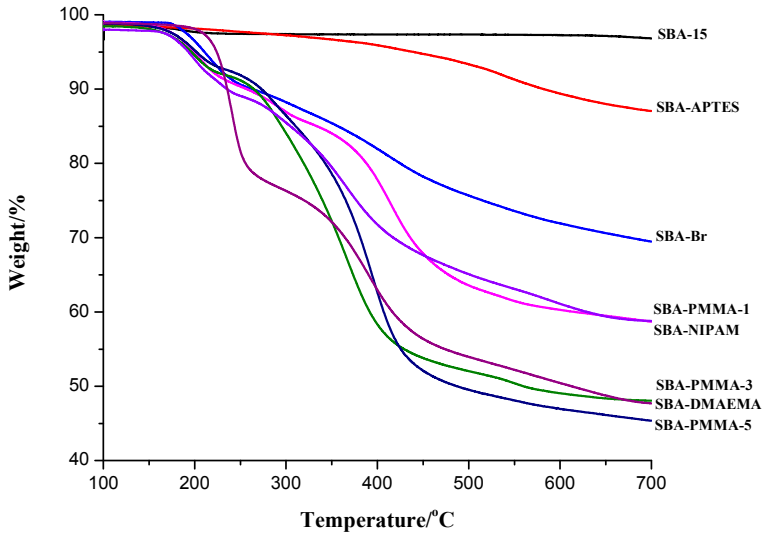

Figure 3. TGA curves of (a) SBA-15, (b) SBA-APTES, (c) SBA-Br, (d) SBA-PMMA, (e) SBA-DMAEMA, and (f) SBA-NIPAM. TGA was performed under the protection of N_2 at a heating rate of 10 ℃ min^{-1}.

One of important properties of mesoporous materials is the porous structure. Thus, in order to investigate the effect of surface grafting on the porous structure, the N_2 adsorption-desorption isotherms of polymer grafted SBA-15 materials together with the pure-silica SBA-15 sample were characterized. The results were shown in Figure 4. The BET surface area (S_{BET}) and total pore volume (V_{total}) were given in the inset Table in Figure 4. The pure-silica SBA-15 sample displayed a type IV isotherm with H1 hysteresis and a sharp increase in volume adsorbed at $P/P_0 \approx 0.78$ with pore volume of 1.09 cm^3/g, characteristic of highly ordered mesoporous materials. For samples SBA-APTES, SBA-Br, and SBA-PMMA-1, they all exhibited a type IV isotherm with a H1 hysteresis loop with lower specific area and slightly smaller pore volume in comparison with SBA-15, e.g. 0.73, 0.45, and 0.17 cm^3/g respectively. However, increasing the amount of PMMA from grafting ratio of 12.5% in SBA-PMMA-1 to 27.6% in SBA-PMMA-5 on the surface of SBA-15, the shape of curve was changed with the pore volume only 0.04 cm^3/g. The surface area also decreased dramatically after the introducing of PMMA polymer chain, e.g. from 594.4 m^2/g of prism SBA-15 to 86.8 and 11.4 m^2/g of SBA-PMMA-1 and SBA-PMMA-5. The above physisorption data indicated that, in the presence of a relatively low grafted density, the textural properties of SBA-15 were substantially maintained. The pore volume was decreased with the increasing amount of introduced PMMA, which was due to the polymer occupied the pore volume.

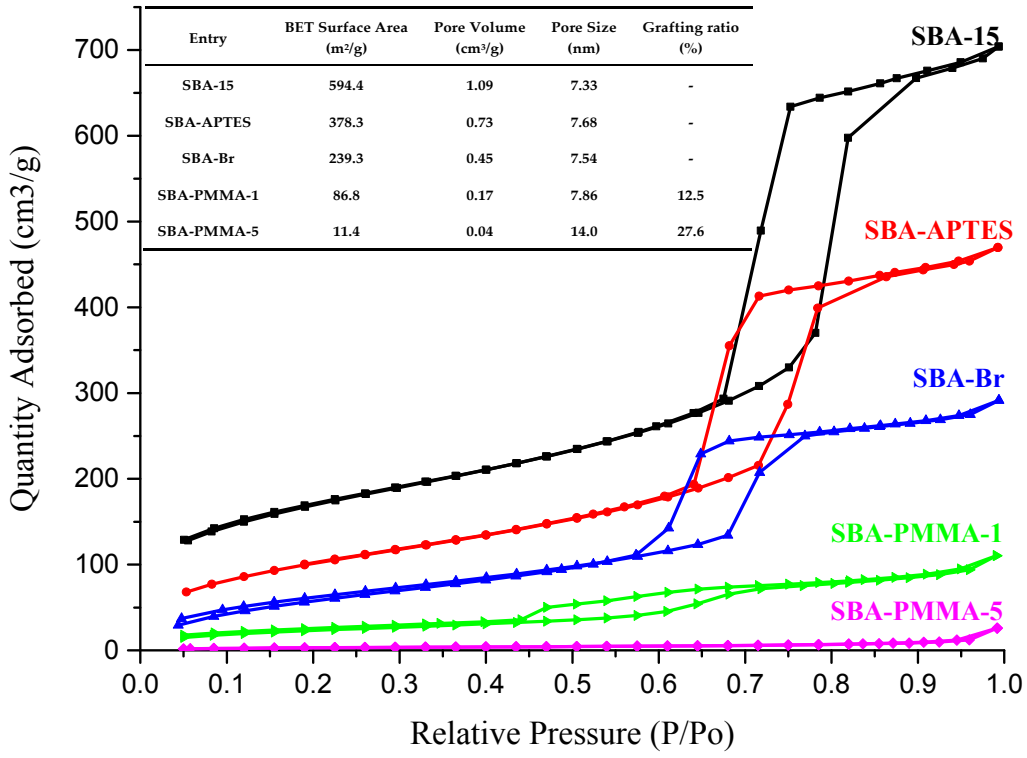

Figure 4. N_2 adsorption-desorption isotherms of (a) SBA-15, (b) SBA-APTES, (c) SBA-Br, (d) SBA-PMMA-1, and (e) SBA-PMMA-5.

The occupy of polymer in pore of SBA-15 after polymerization was verified by the TEM images before and after the polymerization. The TEM images of the pure-silica SBA-15, SBA-APTES, SBA-Br, and SBA-PMMA-5 were compared in Figure 5. The ordered arranged pore arrays of the pure-silica SBA-15 could be clearly seen (Figure 5a). Such ordered pore arrays gradually disrupted after the introducing of APTES and Br onto the surface of SBA-15. The situation was obvious after the introduction of PMMA onto the surface. However, most of such ordered structure could be remained by controlling the amount of introduced polymer, which was easy to realize by using SI-ATRP technique. This results agreed well with the results observed in BET characterization, which showed that low BET surface area of SBA-PMMA with high grafted density.

Peer-reviewed version available at Polymers 2017, 9, 58; doi:10.3390/polym9020058

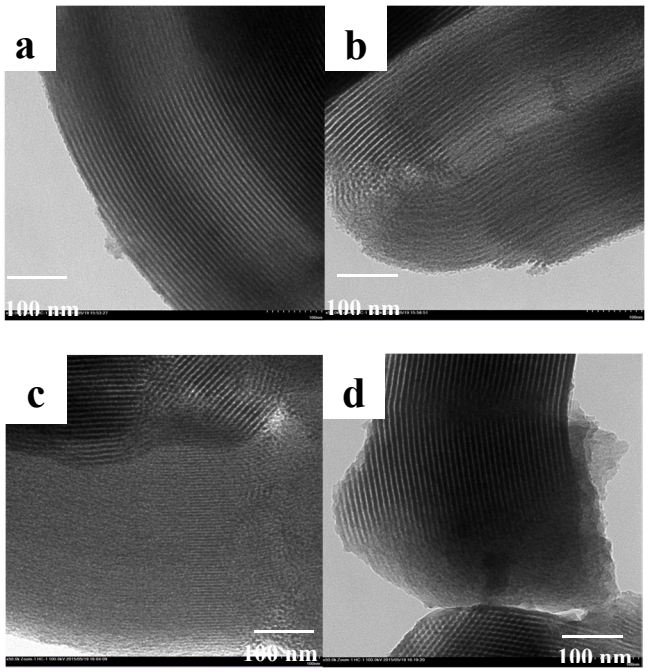

Figure 5. TEM images of (a) pure-silica SBA-15, (b) SBA-APTES, (c) SBA-Br, and (d) SBA-PMMA-5.

The effect of such modification on the ordered structure of SBA-15 was further monitored by XRD characterization. Figure 6 showed the powder XRD patterns of pure-silica SBA-15, SBA-APTES, SBA-Br, and PMMA grafted SBA-15 samples. It showed that the pure-silica SBA-15 exhibited three well-resolved XRD peaks in the region of $2\theta = 0.5 - 2.0°$, which can be indexed to the (100), (110), and (200) diffractions. The peak positions for the samples remained constant after the amine-functionalization process, suggesting high stability of the materials. However, after treating with BMPB and grafting with PMMA, a decrease in diffraction peak intensity was observed, indicating the decrease of crystallinity in the materials. These peaks even disappeared after introducing high amount of PMMA on the surface of SBA-15. As the results, combine the results obtained from BET, TEM and XRD, the textural properties of SBA-15 could be changed from ordered structure to disordered structure after introducing different amount of polymer. It was important to control the amount of polymer introduced onto the surface of SBA-15 for maintaining the ordered structure of SBA-15.

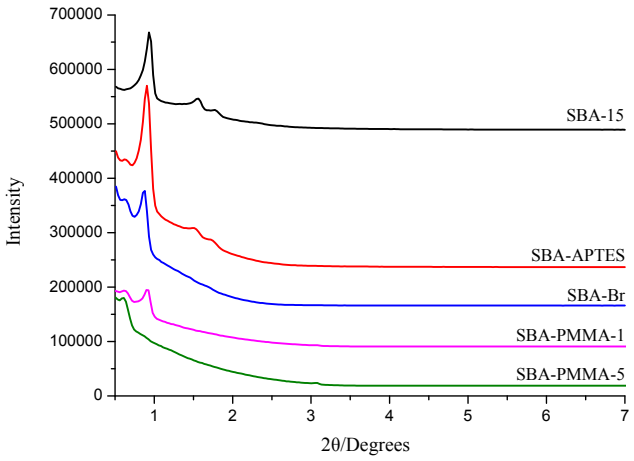

Figure 6. The small and large angles of powder XRD patterns of SBA-15, SBA-APTES, SBA-Br, SBA-PMMA-1 and SBA-PMMA-5.

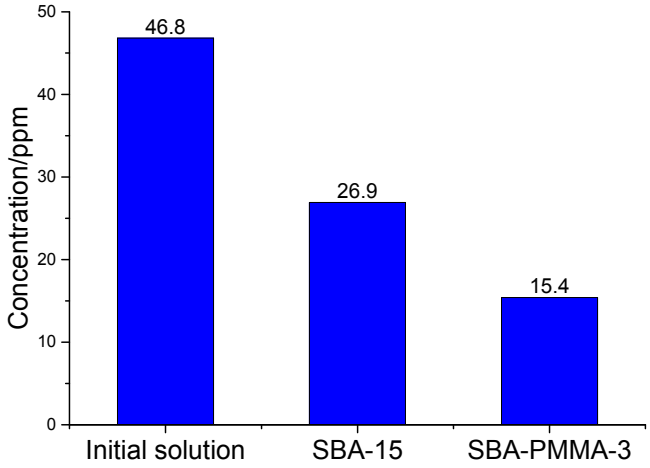

Figure 7. Adsorption abilities of SBA-15 before and after the polymer modification. Conditions: 10 mL of toluene in water solution with concentration of 47 ppm was added with 20 mg adsorbent. The mixture was stirred 24 hrs at ambient temperature.

SBA-15 was widely applied in adsorption materials due to its huge surface area and mesoporous structure. Herein, the adsorption properties of SBA-15 before and after the modification was investigated. Toluene was used as the model adsorbate and aqueous containing 47 ppm of toluene was used as model solution for the adsorption investigation. The results were summarized in Figure 7. It showed that 26.9 ppm of toluene was remained in the solution after the adsorption by pristine SBA-15. The adsorption ability could be improved after using PMMA modified SBA-15, e.g. there was 15.4 ppm of toluene remaining in the solution after using PMMA modified SBA-15 as the adsorbent. Thus, the adsorption properties of SBA-15 could be enhanced by attaching polymer onto the surface.

4. Conclusions

The metal-free photo-induced SI-ATRP of methacrylate on surface of mesoporous SBA-15 has been demonstrated. The polymerization conditions were optimized and using this metal-free photo-induced SI-ATRP, SBA-15 based polymeric composite with adjustable graft density and grafted polymer chain length was obtained. It showed that the porous structure could be modified in range of large scale after the introducing of polymer chain. Enhanced adsorption ability for toluene was obtained after modify SBA-15 with PMMA. This procedure provides a low cost, ready availability, and facile modification way to synthesize the polymeric composites without the contamination of metal with enhanced adsorption ability.

Acknowledgments: This work was supported by the National Natural Science Foundation of China (No. 21306121), the Priority Academic Program Development (PAPD) of Jiangsu Higher Education Institutions and the Program of Innovative Research Team of Soochow University.

References

1. Zhu Y.; Li H.; Zheng Q.; Xu J. and Li X. Amine-Functionalized SBA-15 with Uniform Morphology and Well-Defined Mesostructure for Highly Sensitive Chemosensors To Detect Formaldehyde Vapor. *Langmuir*. **2012**, *28*, 7843-7850.
2. Barbey R.; Lavanant L.; Paripovic D.; Schüwer N.; Sugnaux C.; Tugulu S and Klok H-A. Polymer Brushes via Surface-Initiated Controlled Radical Polymerization: Synthesis, Characterization, Properties, and Applications. *Chem. Rev*. **2009**, *109*, 5437-5527.
3. Moreno J. and Sherrington D. Well-Defined Mesostructured Organic−Inorganic Hybrid Materials via Atom Transfer Radical Grafting of Oligomethacrylates onto SBA-15 Pore Surfaces. *Chem. Mater*. **2008**, *20*, 4468-4474.

4. Wight A. and Davis M. Design and Preparation of Organic–Inorganic Hybrid Catalysts. *Chem. Rev.* **2002**, *102*, 3589-3614.
5. Moller K.; Bein T. and Fischer R. X. Synthesis of Ordered Mesoporous Methacrylate Hybrid Systems: Hosts for Molecular Polymer Composites. *Chem. Mater.* **1999**, *11*, 665-673.
6. Wan Y. and Zhao D. On the Controllable Soft-Templating Approach to Mesoporous Silicates. *Chem. Rev.* **2007**, *107*, 2821-2860.
7. Zhao D.; Huo Q.; Feng J.; Chmelka B. F. and Stucky G. D. Nonionic triblock and star diblock copolymer and oligomeric surfactant syntheses of highly ordered, hydrothermally stable, mesoporous silica structures. *J. Am. Chem. Soc.* **1998**, *120*, 6024-6036.
8. Shi Y.; Meng Y.; Chen D.; Cheng S.; Chen P.; Yang H.; Wan Y. and Zhao D. Highly ordered mesoporous silicon carbide ceramics with large surface areas and high stability. *Adv. Funct. Mater.* **2006**, *16*, 561-567.
9. Liu T.; Jia S.; Kowalewski T.; Matyjaszewski K.; Casado-Portilla R. and Belmont J. Grafting poly (n-butyl acrylate) from a functionalized carbon black surface by atom transfer radical polymerization. *Langmuir* **2003**, *19*, 6342-6345.
10. Liu Y.; Miao X.; Zhu J.; Zhang Z.; Cheng Z. and Zhu X. Polymer-Grafted Modification of Activated Carbon by Surface-Initiated AGET ATRP. *Macromol. Chem. Phy.* **2012**, *213*, 868-877.
11. Husseman M.; Malmström E. E.; McNamara M.; Mate M.; Mecerreyes D.; Benoit D. G.; Hedrick J. L.; Mansky P.; Huang E. and Russell T. P. Controlled synthesis of polymer brushes by "living" free radical polymerization techniques. *Macromolecules* **1999**, *32*, 1424-1431.
12. Devonport W.; Michalak L.; Malmström E.; Mate M.; Kurdi B.; Hawker C. J.; Barclay G. G. and Sinta R. "Living" free-radical polymerizations in the absence of initiators: controlled autopolymerization. *Macromolecules* **1997**, *30*, 1929-1934.
13. Baum M. and Brittain W. J. Synthesis of polymer brushes on silicate substrates via reversible addition fragmentation chain transfer technique. *Macromolecules* **2002**, *35*, 610-615.
14. Pyun J.; Jia S.; Kowalewski T.; Patterson G. D. and Matyjaszewski K. Synthesis and characterization of organic/inorganic hybrid nanoparticles: kinetics of surface-initiated atom transfer radical polymerization and morphology of hybrid nanoparticle ultrathin films. *Macromolecules* **2003**, *36*, 5094-5104.
15. Hui C. M.; Pietrasik J.; Schmitt M.; Mahoney C.; Choi J.; Bockstaller M. R. and Matyjaszewski K. Surface-initiated polymerization as an enabling tool for multifunctional (nano-) engineered hybrid materials. *Chem. Mater*. **2013**, *26*, 745-762.
16. Khabibullin A.; Mastan E.; Matyjaszewski K., and Zhu S. Surface-initiated atom transfer radical polymerization. *Controlled Radical Polymerization at and from Solid Surfaces*: Springer, **2015**. pp. 29-76.
17. Tsujii Y.; Ohno K.; Yamamoto S.; Goto A. and Fukuda T. Structure and properties of high-density polymer brushes prepared by surface-initiated living radical polymerization. *Surface-initiated polymerization I*: Springer, **2006**. pp. 1-45.
18. Fristrup C. J.; Jankova K. and Hvilsted S. Surface-initiated atom transfer radical polymerization—a technique to develop biofunctional coatings. *Soft Matter* **2009**, *5*, 4623.
19. Dalsin J. L.; Hu B-H.; Lee B. P. and Messersmith P. B. Mussel adhesive protein mimetic polymers for the preparation of nonfouling surfaces. *J. Am. Chem. Soc.* **2003**, *125*, 4253-4258.
20. Krishnamoorthy M.; Hakobyan S.; Ramstedt M. and Gautrot JE. Surface-initiated polymer brushes in the biomedical field: applications in membrane science, biosensing, cell culture, regenerative medicine and antibacterial coatings. *Chem. Rev.* **2014**, *114*, 10976-11026.

21. Stuart MAC.; Huck WT.; Genzer J.; Müller M.; Ober C.; Stamm M.; Sukhorukov GB.; Szleifer I.; Tsukruk VV. and Urban M. Emerging applications of stimuli-responsive polymer materials. *Nat. Mater.* **2010**, *9*, 101-113.
22. Sun L, Baker GL, and Bruening ML. Polymer brush membranes for pervaporation of organic solvents from water. *Macromolecules* **2005**, *38*, 2307-2314.
23. Wang J-S and Matyjaszewski K. Controlled/" living" radical polymerization. Atom transfer radical polymerization in the presence of transition-metal complexes. *J. Am. Chem. Soc.* **1995**, *117*, 5614-5615.
24. Kato M.; Kamigaito M.; Sawamoto M. and Higashimura T. Polymerization of methyl methacrylate with the carbon tetrachloride/dichlorotris-(triphenylphosphine) ruthenium (II)/methylaluminum bis (2, 6-di-tert-butylphenoxide) initiating system: possibility of living radical polymerization. *Macromolecules* **1995**, *28*, 1721-1723.
25. Patten TE.; Xia J.; Abernathy T. and Matyjaszewski K. Polymers with very low polydispersities from atom transfer radical polymerization. *Science* **1996**, *272*, 866-869.
26. Matyjaszewski K. and Xia J. Atom transfer radical polymerization. *Chem. Rev.* **2001**, *101*, 2921-2990.
27. Matyjaszewski K. and Tsarevsky NV. Macromolecular engineering by atom transfer radical polymerization. *J. Am. Chem. Soc.* **2014**, *136*, 6513-6533.
28. Pintauer T. and Matyjaszewski K. Atom transfer radical addition and polymerization reactions catalyzed by ppm amounts of copper complexes. *Chem. Soc. Rev.* **2008**, *37*, 1087-1097.
29. Fischer H. The persistent radical effect: a principle for selective radical reactions and living radical polymerizations. *Chem. Rev.* **2001**, *101*, 3581-3610.
30. Treat NJ.; Sprafke H.; Kramer JW.; Clark PG.; Barton BE.; Read de Alaniz J.; Fors BP. and Hawker CJ. Metal-free atom transfer radical polymerization. *J. Am. Chem. Soc.* **2014**, *136*, 16096-16101.
31. Pan X.; Lamson M.; Yan J. and Matyjaszewski K. Photoinduced Metal-Free Atom Transfer Radical Polymerization of Acrylonitrile. *ACS Macro Letters* **2015**, *4*, 192-196.
32. Magenau AJ.; Strandwitz NC.; Gennaro A. and Matyjaszewski K. Electrochemically mediated atom transfer radical polymerization. *Science* **2011**, *332*, 81-84.
33. Theriot JC.; Lim C-H.; Yang H.; Ryan MD.; Musgrave CB. and Miyake GM. *Science* **2016**, *352*, 1082-1086.
34. Discekici EH.; Pester CW.; Treat NJ.; Lawrence J.; Mattson KM.; Narupai B.; Toumayan EP.; Luo Y.; McGrath AJ.; Clark PG.; Read de Alaniz J. and Hawker CJ. *ACS Macro Letters* **2016**, *5*, 258-262.
35. Yan J.; Pan X.; Schmitt M.; Wang Z.; Bockstaller MR. and Matyjaszewski K. Organocatalyzed atom transfer radical polymerization driven by visible light. *ACS Macro Letters* **2016**, *5*, 661-665.
36. Kar M.; Malvi B.; Das A.; Panneri S. and Gupta SS. Synthesis and characterization of poly-l-lysine grafted SBA-15 using NCA polymerization and click chemistry. *J. Mater. Chem.* **2011**, *21*, 6690.
37. Li Q.; Zhang L.; Zhang Z.; Zhou N.; Cheng Z. and Zhu X. Air-tolerantly surface-initiated AGET ATRP mediated by iron catalyst from silica nanoparticles. *J. Polym. Sci. Part A: Polym. Chem.* **2010**, *48*, 2006-2015.